Fluorescence of indirectly excited low vibrational levels of the 1A2 state of sulfur dioxide

ARTICLE *in* THE JOURNAL OF PHYSICAL CHEMISTRY · NOVEMBER 1994

Impact Factor: 2.78 · DOI: 10.1021/j100098a009

4 AUTHORS, INCLUDING:

Fida Al Adel
King Fahd University of Petroleum and Minerals
34 PUBLICATIONS **339** CITATIONS
SEE PROFILE

Mohamed Abdulkader Dastageer
King Fahd University of Petroleum and Minerals
66 PUBLICATIONS **295** CITATIONS
SEE PROFILE

Fluorescence of Indirectly Excited Low Vibrational Levels of the $^1A_2$ State of Sulfur Dioxide

E. Hegazi, F. Al-Adel,* A. Hamdan, and A. Dastageer

Laser Research Section, King Fahd University of Petroleum and Minerals, Dhahran 31261, Saudi Arabia

Received: April 25, 1994; In Final Form: July 28, 1994[⊗]

Vibronic levels of the $^1A_2$ state of SO_2 were excited by crossing a supersonic jet of SO_2 with laser radiation corresponding to cold bands in the 3045−3005 Å region, and the emission spectrum was detected under different laser-jet geometrical alignments. When the exciting laser beam was allowed to cross the jet just outside the spectrometer's field of view, a vibrational fluorescence spectrum of simultaneously excited low $^1A_2$ levels was measured and was found to be independent of the exciting wavelength. This indicated that these levels were populated through inelastic collisions within the jet and that the low-lying $^1A_2$ levels do in general fluoresce back to the ground state. Fourteen band origins near the $^1A_2(0,0,0)' \rightarrow {}^1A_1(0,0,0)''$ transition at 3581 Å were thus identified to within ±1 Å . An excitation spectrum recorded while monitoring the fluorescence of these collision-populated low $^1A_2$ levels showed many cold bands that have not been detected before and also showed that the efficiency of energy transfer due to collisions depended on the initially excited vibronic level.

Introduction

Although there have been numerous reports[1] on the kinetics, spectroscopic, and magnetic properties of the first allowed band (2400−3400 Å) of SO_2, the nature of coupling between the electronic states that absorb and emit radiation in this region is not yet fully understood. This is particularly true for the spectral region around 3050 Å where the magnetic rotation spectrum is maximum.[2] In this region not only the vibronic coupling between the singlet electronic states ($^1A_2$ and $^1B_1$) is important but also the spin−orbit coupling between these states and the nearby existing triplet manifold ($^3B_1$, $^3A_2$, and $^3B_2$), in addition to other possible coupling mechanisms such as the Renner−Teller. The effect of such intricate coupling scheme will be in the splitting of these pure states into many sublevels of different photophysical properties. The task of identifying all of these sublevels is obviously not easy; however, by recognizing the dominant spectroscopic property of these sublevels one may at least identify the pure state that contributes the most in their corresponding total wave functions.

According to the electronic selection rules the only pure (i.e., noninteracting) state that can absorb energy directly from the ground state into the 2400−3400 Å region is the $^1B_1$ state. However, because of the vibronic coupling between $^1B_1$ and $^1A_2$, absorption into the $^1A_2$ state becomes allowed for those vibronic levels that include odd quanta of ν'_3. In fact, it is well-known[3] that absorption into the latter levels has much stronger oscillator strength than absorption into the $^1B_1$ levels (which are diluted because of their vibronic interaction with high-lying $^1A_1$ vibrational levels) and that this strength is attributed mainly to an intensity borrowing mechanism between $^1A_2$ and $^1B_1$. Therefore, for the strong absorption we have

$$^1A_1 + h\nu \rightarrow {}^1A_2{}^n \qquad (1)$$

where n signifies vibrational levels that include odd quanta of ν'_3, (i.e., levels whose vibronic symmetry is A_2a_2). According to Stockburger et al.,[4] the initially produced $^1A_2{}^n$ vibronic levels in eq 1 cannot be those that fluoresce back to the ground state. Therefore, there must be some internal conversion that transfer the excitation to nearby vibronic levels of another electronic state (i.e., $^1B_1$) from which fluorescence emission can occur:

$$^1A_2{}^n \rightarrow {}^1B_1{}^p \quad \text{(rapid internal conversion)} \qquad (2)$$

which is succeeded by processes described by the following branches:

$$^1B_1{}^p + M \rightarrow {}^1B_1{}^q + M \quad \text{(vibrational relaxation)}$$

$$\rightarrow {}^3B_1 + M \quad \text{(collision-induced production of excited triplet } SO_2) \qquad (3)$$

$$^1B_1{}^p \rightarrow {}^1A_1 + h\nu_f \quad \text{(resonance fluorescence)} \qquad (4)$$

$$^1B_1{}^q \rightarrow {}^1A_1 + h\nu_f \quad \text{(background nonresonance fluorescence)} \qquad (5)$$

where p and q signify vibronic levels that may or may not include odd quanta of ν'_3 (p represents only one vibronic level while q represent a few levels below the $^1B_1{}^p$ excited level), and the allowed fluorescence transitions in eqs 4 and 5 all originate from $^1B_1$ levels having quanta of ν'_3 equal to 0, 2, 4, etc.

Many kinetic studies were launched to investigate the various processes that take place after the $^1A_2{}^n$ levels become populated through eq 1, including their quenching through collisions. The study of Stockburger et al.[4] showed that the quenching coefficient was large and that the product state of the quenched $^1A_2{}^n$ levels could not be the $^1B_1$ state. This led Heicklen et al.[1] to suggest that the main channel through which the $^1A_2{}^n$ levels are quenched is vibrational deactivation to the $^1A_2(0,0,0)$ level, which is no longer coupled to the $^1B_1$ manifold and must have a very long lifetime:

$$^1A_2{}^n + M \rightarrow {}^1A_2(0,0,0) + M \qquad (6)$$

A more recent kinetic study was conducted by Koda et al.[5] who investigated the collisional transfer between excited rovibronic levels using SO_2 seeded in a supersonic jet expansion of Ar and/or He. The rovibronic levels that were excited were those of the E band, and their corresponding nondispersed and

* Author to whom correspondence should be addressed.

[⊗] Abstract published in *Advance ACS Abstracts,* October 15, 1994.

0022-3654/94/2098-12169$04.50/0

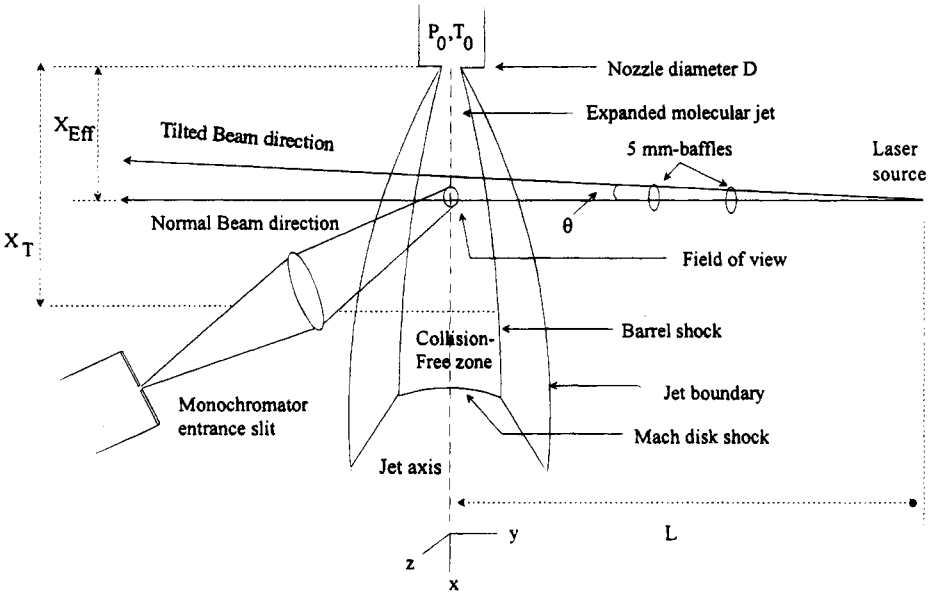

Figure 1. Schematic diagram of a typical supersonic jet expansion showing the two directions of the crossing laser beam. The jet and the detection system are parallel to the x- and z-axes, respectively.

dispersed fluorescence decay, were measured for each line. They confirmed that the main collision process of excited rovibronic levels of $^1A_2$ was not a complete electronic quenching but rather a vibronic energy transfer within the $^1A_2$ state itself, and that the collisionally populated levels had somewhat longer lifetimes. Their study, however, was aimed mainly at investigating the fluorescence transition to the $^1A_1(0,0,1)''$ state, which appears in the resonance fluorescence spectrum of the excited E band, and was not extended to include wavelength-resolved emission spectra from these collisionally excited $^1A_2$ vibronic levels.

In this paper, we present an experiment in which a fluorescence spectrum of this sort has been selectively detected and measured in a supersonic jet expansion. The spectrum was identified to comprise resonance fluorescence transitions from several low $^1A_2$ levels to the ground state, indicating that the $^1A_2^n$ vibronic levels, at least the low-lying ones, do eventually fluoresce back to the ground state. The observed spectrum was also found to be independent of the excitation wavelength within our region of excitation (3050−3000 Å), which confirmed that these low $^1A_2$ levels became populated after molecules in high $^1A_2$ levels had encountered some sort of collisions.

The low $^1A_2$ levels were populated by exciting selected cold bands in the 3050−3000 Å region, followed by subsequent inelastic collisions inside the jet. The detection of the fluorescence from these levels became possible only when the crossing point of the laser beam was excluded from the monochromator's field of view, clearing it from the strong short-lived background and/or resonance fluorescence. Vibrational analysis of these fluorescence transitions was then carried out to identify the band origins of 14 $^1A_2^n \rightarrow {}^1A_1$ bands near the (000)−(000) band at 3581 Å. Also, evidence was found for the presence of many cold vibronic bands in the 3045−3015 Å region that were not detected previously.

Experimental Section

The basic experimental setup and procedure have been described in previous papers.[6,7] In short, nanosecond UV laser pulses of 0.5 cm^{-1} bandwidth, generated by a frequency-doubled ND:YAG-pumped dye laser, was directed perpendicular to a supersonic SO_2 jet beam. The resulting fluorescence emission was then dispersed by a monochromator in a direction perpendicular to both beams, detected by a photomultiplier, and then sent to an EG&G boxcar Model 4402/4422 for signal integrating and averaging. The slit widths of the monochromator were always set at 350 μm, which guaranteed a spectral resolution of ~5 cm^{-1} at 3200 Å. The used SO_2 gas, 99.97% purity (Air Products UK), was seeded in Ar and then allowed to expand through a pulsed valve into a vacuum chamber. The concentration of SO_2 in Ar was fixed at ~0.2% and was measured by a needle valve, whose settings were previously calibrated to a set of known premixed [SO_2]/[Ar] ratios. A pressure oscillation between 10^{-5} and 10^{-6} mbar was maintained in the vacuum chamber as the pulsed valve was oscillating between closing and opening at a constant rate of 10 Hz.

The purpose of seeding SO_2 into the carrier gas was to achieve further rotational cooling. According to the earlier investigations,[6] the rotational and vibrational temperatures become affected in opposite directions when the concentration is varied, and thus these temperatures can be estimated roughly in terms of SO_2 concentration in the jet. In our experiments and at 0.2% concentration the rotational temperature was definitely less than the 10K reported by Kullmer and Demtroder[8] at a concentration of 3%.

A typical schematic diagram of the produced supersonic free jet is shown in Figure 1. The density of Ar and SO_2 mixture, as well as the collision rate and temperature, decreases with increasing distance X until a limit at which these parameters reach their terminal values. The terminal value of X can be calculated[9] from $X_T = 133(P_0D)^{0.4}$, where D is the nozzle diameter of the pulsed valve and P_0 is the carrier gas stagnation pressure. The latter two values were usually kept fixed during the experiment at 300 μm and 3 atm absolute, respectively, which resulted in a fixed value of X_T at 19 mm. The collision-free zone at $X > X_T$ may be considered as the optimum region for crossing the molecular jet with the laser beam. However, to get a reasonable fluorescence intensity the laser beam was directed instead at some distance closer to the pulsed valve (X_{eff} ~ 5 mm), where the molecular collision rate is not negligible.

Under the normal operating conditions, the laser beam, the jet axis, and the detection optics were usually arranged in mutually perpendicular directions. In this case the laser beam was in the normal direction as depicted in Figure 1, which traveled through the center of two light baffles and crossed the

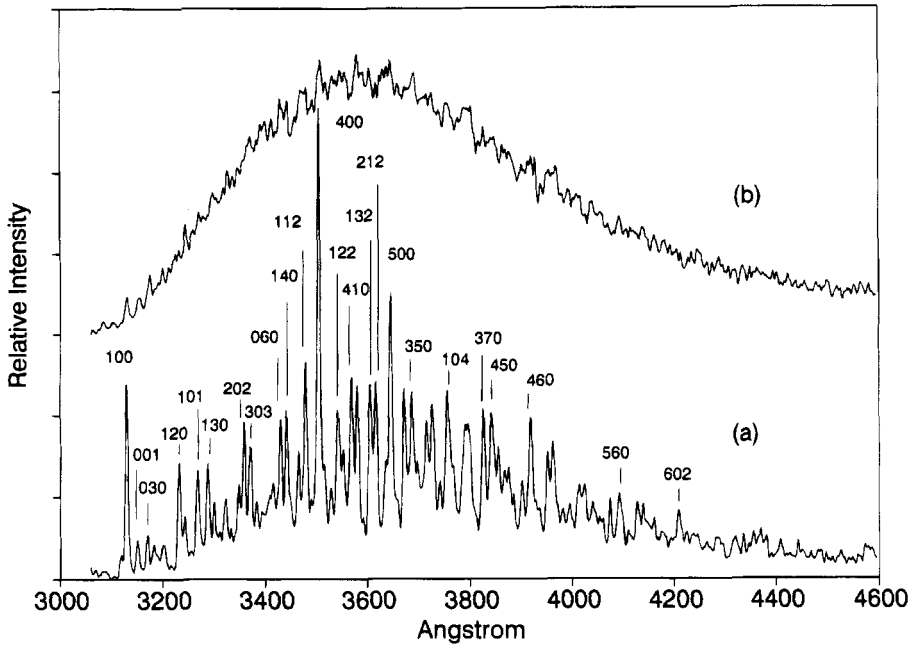

Figure 2. (a) Resonance fluorescence spectrum of the excited F band at 3020.8 Å. The SO_2 concentration was ~0.2% and the nozzle-to-laser distance was 5 mm. The numbers represent the lower vibrational levels of the $^1A_1$ state $(1\nu_1, m\nu_2, n\nu_3)''$ into which some prominent transitions terminate. (b) Background nonresonance fluorescence spectrum excited by the same wavelength but with SO_2 concentration of 100%. Both spectra were measured when the laser beam was in the normal direction.

jet in front of the spectrometer's field of view, allowing the short-lived fluorescence to be detected.

Using the gas number density equation[9]

$$n_X = 0.15 n_0 (X/D)^{-2} \quad (7)$$

the molecular density (n) of the Ar + SO_2 mixture at room temperature was calculated to be $n = 4 \times 10^{16}$ cm^{-3}. Therefore, for the 0.2% SO_2 concentration and at $X_{eff} = 5$ mm (X/D = 17), the partial pressure of SO_2 was ~2.5 mTorr and the total Ar + SO_2 pressure was ~1.2 Torr.

In order to selectively detect long-lived emission one would normally delay the sampling point in the boxcar, and would also shorten the time gate width so that the strong fluorescence signal is excluded from the signal averaging as much as possible. Although this method may work when detecting the long-lived emission from species that are formed immediately after the excitation pulse, it may not prove suitable when detecting the emission from species that need further collisions inside the jet to become excited. To detect the latter molecular species, an alternative method was applied in our experiment, in which the laser crossing point in the jet was directed above the field of view. This was accomplished by tilting the laser beam so that it passed near the edge of the second light baffle. Knowing the distances from the second baffle to the laser source and the jet axis, and assuming that the jet has a typical velocity of 1000 m/s, we calculated that, when the laser beam passes just below the edge of the second baffle, the excited molecules would be detected at least 3 μs after being excited. This delay time allowed the excited molecules to encounter nonnegligible collisions as they traveled downstream the jet. The main collision partners are ground-state SO_2 molecules and/or Ar atoms and the collision rates will be dependent on their corresponding partial pressures at the distances X_{eff}.

In practice, the detection optics were always adjusted to collect the best signal-to-noise ratio and also to avoid the scattered laser radiation. In doing so the position of the field of view would move further down the jet axis (and possibly off-axis also), which would lead to even longer time delays. Unfortunately, because of this fine tuning, the exact position and shape of the field of view could not be specified in our experiment. Nevertheless, it is reasonable to assume that events occurring during the first 3−6 μs after the initial exciting pulse could not be detected in a typically adjusted optical setup.

Results and Discussion

Figure 2 shows two emission spectra of SO_2 excited by the 3020.8 Å laser radiation in an expanded-jet beam. For both spectra the laser beam was in the normal direction such that the point of excitation was exactly in front of the spectrometer's field of view. Figure 2a represents the resonance fluorescence spectrum of the excited F band and was produced with SO_2 concentration of 0.2% and $X_{eff} = 5$ mm, which corresponded to SO_2 partial pressure of 2.5 mTorr and total SO_2 + Ar pressure of 1.2 Torr. Under such low SO_2 partial pressure the collision process in eq 3 will be negligible and the main processes that lead to this emission can thus be described by eqs 1, 2, and 4 solely. This is evident in Figure 2a which includes transitions due to resonance fluorescence only without an appreciable nonresonance background. Shown also in Figure 2a is the identification of the prominent vibrational transitions from the excited upper level to the various ground-state vibrational levels. The vibrational analysis was carried out with 3 cm^{-1} accuracy using the anharmonic expansion of the vibrational energy:

$$G(\nu_1,\nu_2,\nu_3) = \sum_i \omega_i(\nu_i + 0.5) + \sum_{i\le j} x_{ij}(\nu_i + 0.5)(\nu_j + 0.5) + \sum_{i\le j\le k} y_{ijk}(\nu_i + 0.5)(\nu_j + 0.5)(\nu_k + 0.5) \quad (8)$$

where the various vibrational constants of the ground state were taken from the stimulated emission pumping work by Yamanouchi et al.[10] It should be noted that a few transitions were not found to terminate to ground state levels of b_1 vibrational symmetry. Therefore, either the total wave function of the emitting upper level is of mixed vibronic symmetry $B_1b_1 + B_1a_2$, which permits the transitions to terminate to ground-state levels of a_2 vibrational symmetry, i.e., $1\nu''_3$, $3\nu''_3$, $5\nu''_3$, ..., etc., or

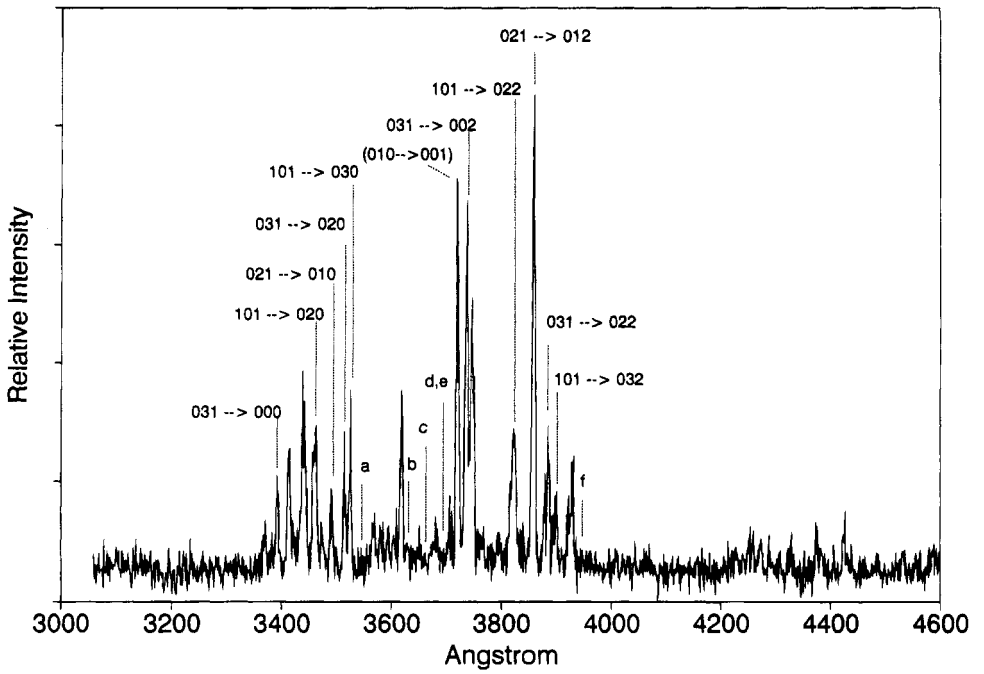

Figure 3. Fluorescence spectrum produced under the same conditions of Figure 2a except that the laser beam was in the tilted position. The spectrum was identified as comprising fluorescence transitions from several low $^1A_2$ vibrational levels into the various vibrational levels of the $^1A_1$ ground state. The ν_3 progressions of a few band systems are identified on the Figure. The letters point at the missing and/or week transitions into the odd ν_3'' levels; (a) $(0,3,1)' \rightarrow (0,0,1)''$; (b) $(1,0,1)' \rightarrow (0,2,1)''$; (c) $(0,2,1)' \rightarrow (0,1,1)''$; (d) $(0,3,1)' \rightarrow (0,2,1)''$; (e) $(1,0,1)' \rightarrow (0,3,1)''$; and (f) $(0,3,1)' \rightarrow (0,0,3)''$.

these transitions originate from different upper vibronic levels that become simultaneously populated through eq 1. An experiment with controlled rotational temperature cooling is currently carried on in our laboratory to answer this question satisfactorily.

As the concentration of SO_2 was gradually increased the intensity of the background fluorescence emission was noticed to increase with respect to the resonance fluorescence spectrum until eventually the latter spectrum was completely immersed inside the intense background fluorescence as shown in Figure 2b. This spectrum was produced when 100% SO_2 concentration was expanded in the jet at 0.9 atm stagnation pressure and X_{eff} = 10 mm. The total SO_2 pressure in this case was ~0.01 Torr and the resulting spectrum can be seen to have similar profile to the one recorded by Strickler and Howell[11] in a closed cell. Such unresolved emission spectrum resulted mainly due to the increased rotational temperature as the concentration was increased, which allowed other vibronic bands to be excited simultaneously by the same laser wavelength. Increased SO_2*–SO_2 collisions may also be responsible for some of the transitions in the unresolved emission spectrum through eqs 1, 3, and 5.

Figure 3 shows a relatively weak emission spectrum recorded under the same experimental conditions as for Figure 2a, (including the exciting wavelength), but with the laser beam tilted in the manner described above. In this case the short-lived strong resonance signal was obscured from the spectrometer's field of view and, consequently, the detected emission must be of molecular species that are either long-lived, or formed after some collision processes, or both. The emission spectrum of Figure 3 was found to be reproducible using other exciting wavelengths such as 3042.8, 3022.6, 3021.0, 3020.8 (F band), 3019.4, 3018.5, and 3016.7 Å , which corresponded to seven cold bands on the excitation spectrum of SO_2. Because of this wavelength independence and the fact that the laser beam was not directed inside the collision-free zone, one can conclude that the emission originated from vibrational levels that became populated due to inelastic collisions.

The vibrational analysis of Figure 3 revealed that these collisionally excited levels were low vibrational levels of the $^1A_2$ electronic state, all of which decayed to the various vibrational levels of the ground state. The procedure used to establish this result depended on the known vibrational anharmonicities of the ground state from ref 10, and the known zero-order vibrational frequencies[3] of the $^1A_2$ state: ν_1' ~780 cm^{-1}, ν_2' ~310 cm^{-1}, and ν_3' ~608 cm^{-1}. Starting from 3380 Å , every relatively strong peak in Figure 3 was first assumed to be a transition to the $^1A_1(0,0,0)''$ level and then a search was made to find whether transitions to the other vibrational levels of the ground state match any peaks in the spectrum at longer wavelengths. If no satisfactory match was found the peak was then assumed to be a transition to the $^1A_1(0,1,0)''$ level and the search for the satisfactory match was repeated, and so on. This lengthy procedure resulted in finding only one transition to the $^1A_1(0,0,0)''$ level whose intensity was relatively strong. This transition occurred at 3394 ± 1 Å , which is known from absorption spectroscopy[3] to be the $^1A_2(0,3,1)' \leftarrow {}^1A_1(0,0,0)''$ transition. The corresponding transitions from the excited $^1A_2$-$(0,3,1)'$ level into $^1A_1(0,1,0)''$, $^1A_1(0,2,0)''$, $^1A_1(1,0,0)''$, $^1A_1$-$(0,3,0)''$, $^1A_1(1,1,0)''$, etc., were found, for example, matching the peaks at 3455 ± 1 Å , 3518 ± 1 Å , 3532 ± 1 Å , 3583 ± 1 Å , 3598 ± 1 Å , etc. Another transition to the $^1A_1(0,0,0)''$ level was found to be at 3430 ± 1 Å , which was much weaker in intensity and was assigned as the $^1A_2$ $(0,2,1)' \rightarrow {}^1A_1(0,0,0)''$ transition since the energy difference was 311 cm^{-1}.

For the other relatively strong transitions above 3380 Å , good fit between observed peaks at longer wavelengths and the calculated positions of the ground-state vibrational levels were found if these transitions were to terminate to levels other than $^1A_1(0,0,0)''$, i.e., to levels such as $(0,1,0)''$, $(0,2,0)''$, $(1,0,0)''$, etc. This is not surprising since, in absorption spectroscopy,[12,3] the longest wavelength transition reported was at 3394 Å , indicating that, at wavelengths above 3394 Å , transitions into

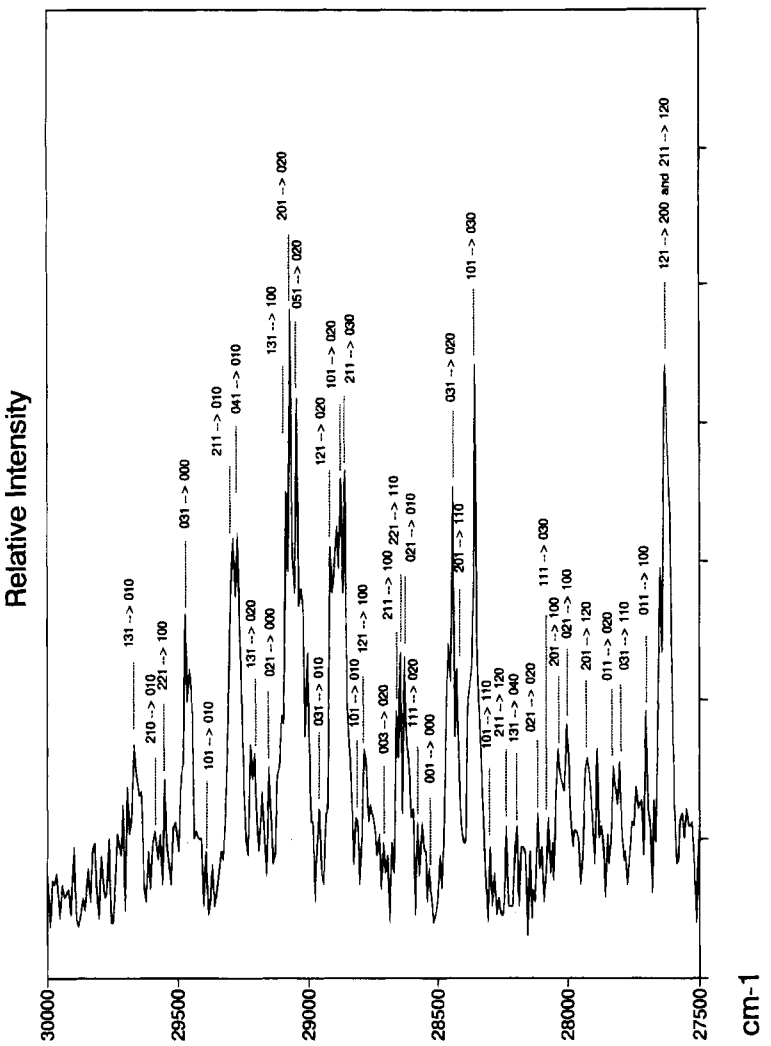

Figure 4. A segment of the fluorescence spectrum showing detailed vibrational analysis. The upper levels of every band system is one of the low $^1A_2$ vibrational bands, while the lower levels belong to the $^1A_1$ ground state.

the $^1A_1(0,0,0)''$ levels are very weak and that the relatively strong transitions in emission terminate only to hot vibrational levels of the ground state. The reason for such very weak cold transitions as we approach the $^1A_2(0,0,0)' \rightarrow {}^1A_1(0,0,0)''$ band may be attributed mainly to the weak Franck–Condon factors in this region as should be expected since the geometrical characters of the $^1A_1$ and $^1A_2$ electronic states are considerably different. As an example of identifying transitions into levels other than $^1A_1(0,0,0)''$, consider the peak at 3527 ± 1 Å. A perfect match between some peaks above 3527 Å and the various transitions to the ground-state levels as calculated from the anharmonicity constants of ref 10 can be found only if the lower level of the 3527 Å transitions is assigned as $^1A_1(0,3,0)''$. Transitions to levels above the $^1A_1(0,3,0)''$ level such as $(1,1,0)''$, $(0,4,0)''$, $(1,2,0)''$, etc., would then match the peaks at 3541 ± 1, 3592 ± 1, 3607 ± 1 Å, etc., while the transition into levels below $(0,0,0)''$ would be considerably weaker. The transition into $^1A_1(0,0,0)''$ in this particular example would be at 3344 Å, and by using the fundamental frequencies of the $^1A_2$ state one could then identify this position to correspond to the $^1A_2(1,0,1)' \rightarrow {}^1A_1(0,0,0)''$ transition.

According to the vibronic selection rules, transitions from levels of A_2a_2 symmetry to levels of B_1a_2 symmetry, such as $^1A_2(0,3,1)' \rightarrow {}^1A_1(0,0,1)''$, should be missing or at least very weak. This situation is evident in Figure 3 in which the $^1A_2(0,3,1)' \rightarrow {}^1A_1(0,0,m)''$ progression, for example, shows alternating strong and missing (or very weak) components depending on whether m is even or odd, respectively. The position of the missing $^1A_2(0,3,1)' \rightarrow {}^1A_1(0,0,1)''$ and $^1A_2(0,3,1)' \rightarrow {}^1A_1(0,0,3)''$ components in this case are denoted by "a" and "f", respectively. Four other examples of this sort are also shown in Figure 3 in which the letters b, c, d, and e mark the positions of the missing transitions into levels of $\nu_3'' = 1$.

A few relatively strong transitions in Figure 3 were also found to match transitions that originate from levels of A_2b_1 symmetry into levels of B_1a_2 symmetry. An example of such transitions is $^1A_2(0,1,0)' \rightarrow {}^1A_1(0,0,1)''$ at ~3721 Å, which is put between brackets on the spectrum. If this situation can be confirmed then one may conclude that upper $^1A_2$ levels that are not coupled with $^1B_1$ through odd ν_3' can also fluoresce to the ground state. However, because Figure 3 contains transitions from several upper levels to several lower levels, such confirmation would certainly require a better spectral resolution that was beyond our experiment's capability. We should also note that during the collisional-induced cascade some levels of $^3A_2$ levels may also become excited and later decay to the ground state with intensities comparable to, at least, those of the decaying noncoupled $^1A_2$ levels. Such mechanism cannot be confirmed also without a better spectral resolution, especially at wavelengths above 4000 Å where the spectrum becomes more congested.

Figure 4 shows a segment of the spectrum in Figure 3 with detailed assignments of the vibrational transitions. The vibrational analysis, carried out to within 0.5 Å spectral resolution,

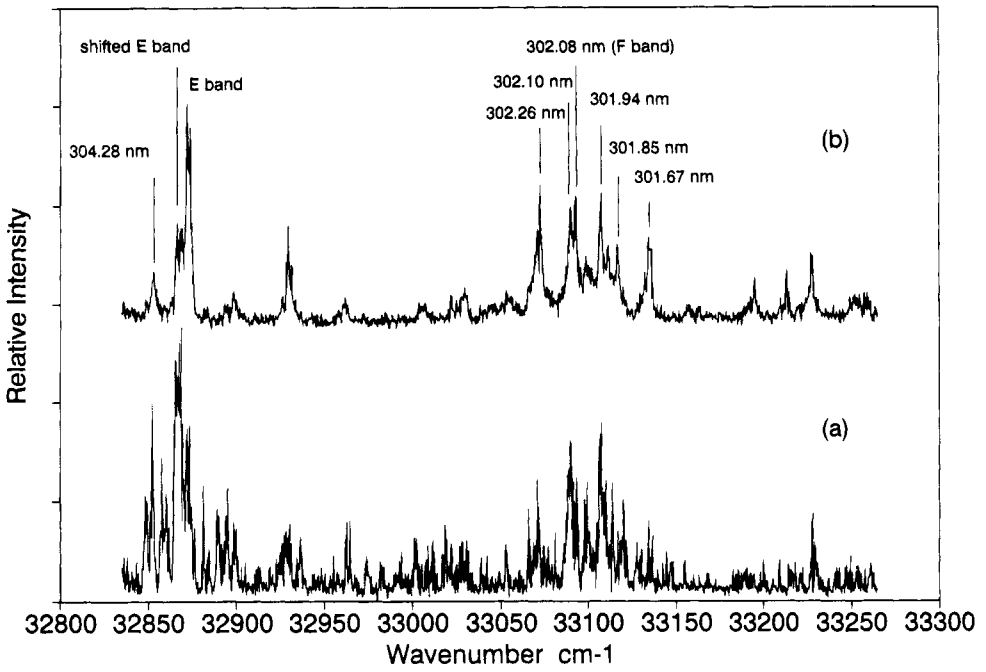

Figure 5. Excitation spectra measured by scanning the laser in the 3045−3005 Å region while monitoring the total fluorescence signal in (b) and the filtered fluorescence signal at 3721 Å in (a). The experimental conditions were the same for both spectra except that the laser beam was in the normal direction in (b) and in the tilted direction in (a). The excitation wavelengths used to produce the fluorescence spectrum of Figure 3 are identified on (b).

TABLE 1: Position of $^1A_2(l,m,n)' \rightarrow {}^1A_1(0,0,0)''$ Transitions Near the Origin of the $^1A_2$ State, and Their Assignments

obsd energy levels (± 12 cm^{-1})	assigned upper $^1A_2$ level (lv_1,mv_2,nv_3)	calcd energy levels (cm^{-1})
28 523	0,0,1	28 525
28 844	0,1,1	28 835
29 146	0,2,1	29 145
29 311	1,0,1	29 305
29 456	0,3,1	29 455
29 741	0,0,3	29 741
29 784	0,4,1	29 765
29 929	1,2,1	29 916
30 079	0,5,1	30 076
30 088	2,0,1	30 085
30 181	1,3,1	30 235
30 395	2,1,1	30 395
30 482	1,4,1	30 544
30 551	1,0,3	30 526

resulted in identifying about 90% of the lines, many of which are shown on the Figure. Once transitions from one upper vibronic level had been identified, eq 8 was then used again to calculate the transition from this upper level into $^1A_1(0,0,0)''$. Fourteen such transitions were calculated to within ± 1 Å and are summarized in Table 1. The identification of the upper $^1A_2$ was based on the $^1A_2(0,0,0)' \rightarrow {}^1A_1(0,0,0)''$ transition being at 3581 Å and on the zero-order values of the vibrational frequency separations of the $^1A_2$ state as given by Hamada and Merer.[3]

The above results provide a spectroscopic evidence that excited $^1A_2$ vibronic levels, at least in the spectral region of maximum magnetic rotation, undergo a cascade decay upon collisions. During this cascade, levels that become successively populated fluoresce back to the ground state with relative intensities according to the usual Franck-Condon factors. These results are in agreement with the second mechanism brought forward by Koda et al.[5] to explain the fluorescence transition into the $^1A_1(0,0,1)''$ level when the E band was excited. The mechanism assumed collisional excitation of a_2-symmetry vibronic levels (i.e., A_2b_1) along with b_1 levels (i.e., A_2a_2). In their work, these collisionally excited levels were confined to levels that were very close to the E band's upper level and were responsible for the fluorescence into the $^1A_1(0,0,1)''$ level. In the present work, the collisionally excited $^1A_2$ vibronic levels are >5000 cm^{-1} below the initial exciting energy, which indicates the involvement of several cascading collisions rather than a single one.

The results also suggest that, in addition to eq 2, the immediate fate of an initially excited $^1A_2^n$ level, especially a low-lying one, may also be a direct fluorescence:

$$^1A_2^n \rightarrow {}^1A_1 + h\nu \qquad (9)$$

The branching ratio of this process, however, should be small since the overall intensity of Figure 3 is about 10 times weaker than that of Figure 2.

Figure 5 shows a comparison between two excitation spectra of SO_2 in the region of maximum rotation spectrum. Both spectra were produced with SO_2 concentration of ~0.2% but with different optical alignments and different monitored fluorescence signals. In the excitation spectrum of Figure 5b the laser beam was in the normal position as shown in Figure 1, and the spectrum was produced by scanning the dye laser and monitoring the total fluorescence signal (i.e., no monochromator was used). For the excitation spectrum of Figure 5a, on the other hand, the laser beam was in the tilted position and the spectrum was produced by scanning the dye laser while monitoring the filtered fluorescence of the $^1A_2(0,1,0)' \rightarrow {}^1A_1(0,0,1)''$ at ~3721 Å . The aim was to identify those upper vibronic levels that eventually become relaxed to low $^1A_2$ (and/or $^3A_2$) levels after later inelastic collisions. Because the laser beam was in the normal position the detection will favor the short-lived fluorescence signal and, therefore, the excitation spectrum in Figure 5b will represent those excited $^1A_2^n$ vibronic levels that are seen mainly through the resonance fluorescence emission. In other words, those $^1A_2^n$ levels that undergo the successive processes of eqs 2 and 4 immediately after being excited. The excitation spectrum in Figure 5a, on the other hand, represents those vibronic levels that are seen mainly

through the fluorescence of the collisionally excited low $^1A_2$ (or $^3A_2$) levels. i.e., those levels whose final fate can be described by the following sequence of events:

$$^1A_2{}^n + M \rightarrow {}^1A_2{}^L + M \quad \text{(cascade to an emitting low-lying singlet level)}$$

$$\rightarrow {}^3A_2 + M \quad \text{(cascade to an emitting triplet level)} \quad (10)$$

$$^1A_2{}^L \rightarrow {}^1A_1 + h\nu_f \quad \text{(resonance fluorescence)} \quad (11)$$

or

$$^3A_2 \rightarrow {}^1A_1 + h\nu_p \quad \text{(resonance phosphorescence)} \quad (12)$$

where the superscript L signifies low vibrational levels.

There are two main differences between Figures 5, a and b. The first is that there are more vibronic bands in spectrum a than there are in spectrum b, all of which are cold bands that have not been seen before. The upper levels of these cold bands must have long lifetimes since they could not be detected in Figure 5b. The density of these cold bands is larger than what would be expected from the vibrational levels of only a pure $^1B_1$ state, since the $^1B_1(0,0,0)-{}^1A_1(0,0,0)$ is at about 3200 Å (31 240 cm^{-1}) and the $^1B_1$ values of ν_1 and ν_2 are 690 and 460 cm^{-1}, respectively. Also since the density of a_2-symmetry levels of $^1A_2$ is about 0.05/cm^{-1} in this region and not >1/cm^{-1} as seen in Figure 5a, one may also exclude the possibility that the cold bands in Figure 5a belong to the pure $^1A_2$ state. The high density of levels in Figure 5a may therefore be explained[8,14] as a result of splitting that occurs due to an intricate coupling scheme between the $^1A_2$ and $^1B_1$ on one side and the triplet manifold in the region (i.e., the $^1B_3$, $^3A_2$, and $^3B_2$ states) on the other side, in addition to a possible Renner–Teller coupling, which involves high vibrational levels of the ground state:

$$\Psi_k = \alpha_k(\sum_i a_i\Psi_i(^1A_2) + b\Psi(^1B_1)) + \sum_i \beta_{kj}\Psi_j(^1A_1, {}^3B_2, \ldots) \quad (13)$$

where α and β are coefficients that depend on the energy separations between the levels of the coupled $^1A_2$ and $^1B_1$ states and on the perturbing levels.[14]

The second difference between Figures 5, a and b, is in the relative intensities. The intensity pattern in Figure 5a is very different from that of Figure 5b, even for those bands that appear in both spectra such as the group of bands near the F and E bands. The upper level that become populated when the E band is excited, for example, does not seem to transfer its energy to the other $^1A_2$ levels as efficiently as the upper level of the shifted E band does. The same can be said about the F band at 3020.8 Å and its neighbor at 3021.0 Å , respectively. Therefore, the efficiency of the energy transfer due to collisions depends on the initially excited vibronic level, or more accurately, on the excited rotational level, since different rotational levels of the some vibronic state behave kinetically different.[15]

Finally, we note that, because some $^1A_2$ vibronic levels can become populated through collisions and later fluoresce back to the ground state, any measurement of excitation spectrum will depend strongly on the preset time parameters of the detection equipment such as the sampling point and the gate width. It is very probable then that the many faint lines seen in the excitation spectra of the cold bands, such as the E band,[7,14] originate from collisionally excited vibronic levels and that their intensities may be enhanced by proper delayed detection.

Summary and Conclusion

A method based on changing the laser beam alignment has been used in a supersonic jet to favor the detection of fluorescence from collisionally excited SO_2 vibronic levels. The initially excited $^1A_2{}^n$ levels in the 3045–3005 region Å were found to cascade to lower vibrational levels of the same electronic state and at the same time fluoresce back to the ground state during the cascade. The resulting fluorescence spectrum showed appreciable intensity in the 3370–4000 Å region and was found to be composed of transitions from several low-lying $^1A_2{}^n$ vibrational levels. Fourteen band origins near the $^1A_2$-$(0,0,0)' \rightarrow {}^1A_1(0,0,0)''$ transition at ~3581 Å have thus been identified by vibrational analysis and are listed in Table I. This result indicates that, besides the rapid internal conversion of eq 2, branching into eq 9 may in general occur. This is particularly true for the low-lying $^1A_2{}^n$ levels, at which the density of pure $^1B_1$ levels are scarce. It is possible that during the cascade transitions from b_1-symmetry levels of the $^1A_2$ state and/or levels from the $^3A_2$ state become excited and decay down to the ground state as well. An experiment with better spectral resolution will be needed, however, to sort out the transitions from the $^3A_2$ state and shed light on its vibrational constants. The excitation spectrum recorded while monitoring the fluorescence signal from the collisionally excited low-lying $^1A_2$ levels showed the presence of many cold bands that were not previously known and also showed that the upper levels of these bands seem to have longer lifetimes and become depopulated through collisions before emitting. The relative intensities of the bands in the latter excitation spectrum were also found to be different from those of the excitation spectrum produced by monitoring the short-lived fluorescence signal, which indicates that the efficiency of the collision process in eq 10 may depend on the initially excited rovibronic level.

Acknowledgment. Support from the Research Institute of KFUPM is greatly appreciated.

References and Notes

(1) Heicklen, J.; Kelly, N.; Partymiller, K. *Rev. Chem. Intermed.* **1980**, *3*, 315 (and references therein).
(2) Brus, L. E.; McDonald, J. R. *J. Chem. Phys.* **1974**, *61*, 97.
(3) Hamada, H.; Merer, A. J. *Can. J. Phys.* **1974**, *53*, 2555.
(4) Stockburger, L; Braslavsky, S; Heicklen, J. *J. Photochem.* **1973**, *2*, 15.
(5) Koda, S.; Yamada, H.; Tsuchiya, S. *J. Phys. Chem.* **1988**, *92*, 383.
(6) Al-Adel, F.; Hamdan, A.; Binbrek, O; Baskin, J. S. *Chem. Phys. Lett.* **1992**, *189*, 23.
(7) Hegazi, E.; Hamdan, A.; Al-Adel, F. *Chem. Phys. Lett.* **1994**, *221*, 33.
(8) Kullmer, R.; Demtroder, W. *Chem. Phys.* **1985**, *92*, 423.
(9) Anderson, J. B.; Fenn, J. B. *Phys. Fluids* **1965**, *8*, 780. See also Skinner, A. R.; Chandler, D. W. *Am. J. Phys.* **1980**, *48*, 8.
(10) Yamanouchi, K.; Takeuchi, S.; Tsuchiya, S. *J. Chem. Phys.* **1990**, *92*, 4044.
(11) Strickler, S. J.; Howell, D. B. *J. Chem. Phys.* **1968**, *49*, 1947.
(12) Brand, J. C. D.; Nanes, R. *J. Mol. Spectrosc.* **1973**, *46*, 194.
(13) Shaw, R; Kent, J.; O'Dwyer, M. F. *J. Mol. Spectrosc.* **1980**, *82*, 1.
(14) Kullmer, R.; Demtroder, W. *J. Chem. Phys.* **1984**, *81*, 2919.
(15) Holtermann, D. L.; Lee, E. K. C.; Nanes, R. *J. Chem. Phys.* **1982**, *77*, 5327.